P R E P R I N T – ICPWS XV
Berlin, September 8–11, 2008

Corrosion Product Sampling in Power Plants under Water/Steam Cycle Conditions

Piti Srisukvatananan[a], Derek H. Lister[a], Chien-Ee Ng[a], Robert Svoboda[b] and Karol Daucik[c]

[a]Department of Chemical Engineering, University of New Brunswick, Fredericton, Canada
[b]Materials Department, Alstom, Baden, Switzerland
[c]Dong Energy, Fredericia, Denmark
E-mail: j587k@unb.ca

Sampling of process systems is important in power plants because operating decisions often rely on water chemistry information. To obtain representative samples, a properly designed sampling system must take into account many factors. Sponsored by the International Association for the Properties of Water and Steam (IAPWS), an international collaboration among the University of New Brunswick, Canada, Alstom, Switzerland and Dong Energy, Denmark produced a comprehensive review of sampling techniques in nuclear and fossil power plants. This paper, reporting continuing work, includes a study on isokinetic sampling issues. A Computational Fluid Dynamics (CFD) program was used to assess the collection efficiency for magnetite particles of sampling nozzles under water- and steam-cycle conditions. The effects of types of sampling nozzle and the velocities within the nozzle opening were investigated. It is shown that for sampling magnetite particles from steam, where the fluid viscosity is low, the collection efficiency significantly depends on sampling velocity. Any practical sampling nozzle acts as an obstacle that disturbs the flow field and tends to remove the isokinetic condition. Although deviations from ideal sampling are small, in steam it is advisable to sample at appropriate rates. In liquid, sampling velocity has almost no effect within the ranges of the parameters studied.

Introduction

Sampling is of importance in power plant process systems since operating decisions often rely on water chemistry information. Experience has shown that unrepresentative samples can mislead operating personnel and result in poor chemistry control. Representative samples are also necessary in studies of corrosion and corrosion product transport.

Attention is often focused on the analytical instrument; however, to obtain representative samples, a properly-designed sampling system and an appropriate procedure must be employed. The critical factors to ensure representative samples are: location of sampling points, material selection of sampling system, sampling system design, sampling procedures and handling of samples after extraction to maintain the integrity of the sample prior to analysis.

An international collaboration among the University of New Brunswick, Canada, Alstom, Switzerland and Dong Energy, Denmark was sponsored by IAPWS (the International Association for the Properties of Water and Steam). It resulted in a comprehensive review of sampling techniques in nuclear and fossil power plants [1]. The report included theoretical and practical aspects. It pointed out that difficulties in achieving representative samples arise when there are temperature and phase changes. Major sources of sampling deficiencies are deposition in the sample line, valves and coolers, and release of deposited material. To minimize such errors, attempts have been made to explain mechanistically sampling discrepancies in terms of deposition and dissolution phenomena. It should be noted that in some cases, an error can be attributed to anisokinetic sampling, which is largely discussed in this paper.

Particle Transport

There are different processes controlling particle transport. These are diffusion, thermophoresis, turbulence, gravity, electrical and Van der Waals forces. The significance of each force depends upon the properties of the fluid, the particle and the pipe wall. The net effect of these forces can cause particle deposition.

It is believed that over time, equilibrium between particle deposition and re-entrainment is established as long as velocity and other physical pa-

rameters are kept constant. Beal [2] proposed that turbulence increases deposition because eddies created in turbulent flow enhance mass transfer to the surfaces. However, as turbulent intensity increases to a certain point, eddies will no longer increase net deposition because increased wall shear stress will promote removal of deposited particles. Based on Beal's model, for 5-μm particles flowing in liquid at 1.8 m/s (6 ft/s) and 121°C (250°F), equilibrium will be established after a month.

It is shown in [1] that Beal's model may not be entirely definitive especially when particles approach the wall where other forces become important. These forces are lift and drainage forces, which predominate in liquid systems but not in gas systems. In addition, the effects of surface roughness, thermophoresis, heat flux and surface charge on particle deposition should be considered. The last is known to be significant, particularly for small particles in liquid systems.

Soluble Species Interaction in Sample Lines

Soluble species in the circuit can interact with sample lines by incorporating into the oxide films formed on the surfaces. The rate of incorporation is governed by the growth of the film which, in turn, is governed by the corrosion of the base metal and deposition of particles.

Ionic species also interact with particles suspended in the circuit via dissolution and precipitation processes. If the solution is under-saturated, dissolution will take place. The solution can also become over-saturated during cooling, resulting in particle growth and precipitation on sample line walls or in the cooler.

The study of corrosion product sampling from the Sizewell B PWR primary coolant indicated that soluble corrosion products are subject to sample line effects caused by deposition on sample line walls when coolant was sampled hot [3]. The same study also pointed out that the deposition of soluble species can occur at temperatures above 120°C, below which deposition problems disappear. If sample line walls are preconditioned, measurements of soluble corrosion products are unlikely to be affected by corrosion product release.

In reality, sample lines can be very long (up to 300 m) because of the use of one or more centralized sampling units in a power plants. A long sample line provides a considerable inventory of material that could be held up, and a portion of this inventory can be returned to the sample flow by transients in flow or chemistry. Local sampling stations can avoid such sample line effects.

Soluble species not only react with sample line walls and components but also adsorb on oxide particles. It was found that magnetite can retain up to 3.4 $\mu g/cm^2$ of impurities, such as sodium, after only 24 hour exposure to superheated steam [4]. In order to obtain a representative soluble concentration, therefore, representative particle sampling is also required.

Particle and ionic transport at elevated temperatures are complex processes. Mechanisms attributed to deposition on system walls are: crystallization resulting from solubility changes, settling resulting from gravity and hydrodynamic forces, and electrostatic attraction between particles and the tube wall. In general, the relationships among most parameters can be explained qualitatively. Quantitative analysis, however, seems to be system-dependent.

Sampling System and Procedures

Sampling system design and procedures to obtain representative samples are recommended as follows [1]:

- Sample lines should be as short as possible to reduce lag time and possible interactions between samples and sample lines.
- Maintaining turbulence in the sample line seems advisable and, hence, Reynolds number is the key criterion. The evaluation of the Reynolds number should be made all along sample lines since changes in fluid properties are expected in high-temperature sampling systems.
- Sample lines should be of the smallest practicable bore to minimize sample amount yet provide adequate turbulence. If possible, they should be able to operate under a range of system operating loads: full load, low load and guaranteed overload. In some cases, capillary tubing is used. Major advantages of capillary tubing are that it acts as a pressure reducing device, eliminating the need of other pressure-controlling devices, and is capable of delivering a small amount of flow while maintaining turbulence in the line. Experience has shown that capillary tubing is susceptible to blockage; however, this problem is strongly related to crud level and corrosion product size.
- Sample systems should contain as few valves, fittings and sharp bends as possible.
- Sample lines and other components should be made of inert materials.

- Sample flow rate should be kept constant and flow should be continuous during sampling. Changing sample flow rate changes Reynolds number and the temperature profile in the sample line which, in turn, changes the deposition/dissolution properties.
- Samples should be taken over a period of time to be statistically representative.
- Sampling points should be selected in areas where uniform distribution of all phases in the system is established.
- Sample line flushing is recommended for grab samples.
- Following a change in sample flow rate or sample line flushing, sufficient time must be given to avoid the resulting transient in concentration. An appropriate waiting time for decay of particulate transients for each system should be determined individually by taking particulate measurement as a function of time.
- Sampling during load changes (startup or shutdown) is the most challenging because the transients never allow steady state in the sample line to be established. The best alternative is to have local sampling systems (short sample lines) in which interactions between the sample and the sample line are kept to minimum. It should be noted that a crud burst is usually observed during a startup. If sample line blockage is anticipated, a larger diameter sample line is suggested. Continuous chemistry surveillance is needed, and manual adjustment of sample flow rate is suggested if isokinetic conditions are required.
- Handling and analysis after sample extraction must be cautiously performed to avoid errors. Allow as short a time as possible between collection of a sample and its analysis. Some samples need to be preserved. Other special precautions should be taken for particular constituents. For instance, the exposure of samples to air prior to analysis can markedly affect the concentrations of soluble and insoluble species, as observed at an operating nuclear station [5].

Sampling Nozzles

The sampling nozzle is one of the main components of sampling systems. There are a number of types of sampling nozzle available in the market. The design and installation are meant to extract samples representatively. It has been found, however, that representative samples are not necessarily obtained [1]. Nonetheless, the nozzles can provide consistent results which are useful in terms of detecting concentration changes. To obtain representative results, sampling nozzles should be installed facing upstream and, if possible, located where all the phases are uniformly distributed. Representative sampling of non-uniform phase distributions can be difficult to achieve in two-phase steam. Since there is a significant portion of liquid phase traveling as a water film on the wall, a steam sample extracted from the bulk therefore contains too little liquid. The previous ASTM Standards suggested a multiport sampling nozzle [6], which was intended to sample fluids in correct proportion over the whole cross-section of the pipe. This nozzle, however, is not included in the latest ASTM Standards [7].

Isokinetic Sampling

Isokinetic sampling has been widely employed and recommended as one of the key techniques to obtain representative samples of suspended particles. This requires the fluid entering the sampling nozzle to have the same velocity (speed and direction) as the main stream. As a result, the primary (e.g. fluid) and secondary (e.g. particles) phases flowing towards the sampling nozzle are collected in the correct proportions. If sampling velocity is too low, because of their inertia, heavy particles can enter a nozzle, even if the streamline on which they are located passes by the nozzle. Hence, too many particles are collected, resulting in too high a particle concentration. On the other hand, if the sampling velocity is too rapid, particles again fail to adhere to the streamlines and end up bypassing the nozzle. In that case, too few particles are collected, resulting in too low a particle concentration.

It is evident, however, that truly-isokinetic sampling has been compromised in many cases, yet meaningful results can still be obtained [8]. It has been suggested that isokinetic sampling is necessary in two-phase flow if the Stokes number is greater than 0.01 [9]. The Stokes number is an indicator of particle persistence in a flow stream with respect to some obstacle, and can be calculated as follows:

$$Stk = \frac{\rho_p d^2 U_0}{18 \mu D_s} \quad (1)$$

where ρ_p is the particle density, d is the particle diameter, U_0 is the free stream velocity, μ is the fluid viscosity and D_s is the sampling nozzle diameter. In other words, it indicates the ability of a particle to adjust itself to a new force field by taking into account particle density, particle diameter,

fluid viscosity and fluid velocity. It has been reported that it is advisable to sample 1-μm magnetite particles isokinetically in air and steam conditions, since viscosities of those media are fairly low, resulting in Stokes numbers greater than 0.01 [1]. On the other hand, isokinetic sampling is not necessary in water systems in which the medium has much higher viscosity and Stokes numbers are typically about 0.002.

To improve our understanding of such issues of isokinetic sampling, a commercial Computational Fluid Dynamics (CFD) program is used to evaluate the collection efficiency for magnetite particles in sampling nozzles under water- and steam-cycle conditions. An Eulerian-Eulerian multiphase model is employed to determine particle concentrations in different types of sampling nozzle. In addition, CFD simulations provide insights into the effect of the nozzle on the flow field and into particle behavior around nozzles.

Simulations of Sampling Nozzle Collection Efficiency

Nozzle Types and Their Geometry

There are 3 types of sampling nozzle in this study: Ideal Nozzle, Nozzle A and Nozzle B as illustrated in Figures 1 to 3. All of the nozzles have the same bore diameter of 4.42 mm, the inner diameter of standard ¼ in. tube. The Ideal Nozzle is equipped with an 88.4-mm-long entering port, which has a base-wall thickness of 0.97 mm and a knife-edged opening at the end. It is considered as an ideal nozzle since a long entering port makes the flow field at the actual sampling point undisturbed by the nozzle body. Knife-edged openings also provide the smallest possible disturbing effect on the flow field. It should be noted that the Ideal Nozzle is only hypothetical. It is not practical because such a long entering port with a knife-edge entrance could not be made strong enough and would be difficult to install. For the purpose of this study, the Ideal Nozzle is introduced as a benchmark. Nozzle A follows a commercial nozzle design; a cylindrical shape, 10 mm in diameter and 36.78 mm in length. Ideal Nozzle and Nozzle A have the same nozzle body geometry. Nozzle B mimics a recently-developed sampling nozzle. It has a conical shape with a tip protruding from the nozzle body, as shown in Figure 3. It has a base diameter of 33.69 mm and protrudes from the pipe wall 23.99 mm, which is less than the protrusion of Ideal Nozzle and Nozzle A. The wall thickness of the entering port is 0.97 mm.

As shown in Figures 1 to 3, the computational domains are three-dimensional, half pipes. Entering ports of all sampling nozzles face the flow direction (y+ direction) and their center is located at 0.12 of pipe diameter from the pipe wall as suggested in ASTM 1066-06 [7]. The diameter of the main pipe is 155 mm. The distance of the pipe inlet upstream of the nozzle is set to ensure that distribution of all phases is uniform and not disturbed by the nozzle at the domain inlet. The outlet is placed at a distance downstream of the nozzles, far enough to avoid the recirculation zone behind the nozzle. This is important in simulations only in terms of computational instability. In this study, the distance from the middle of the nozzle to the pipe outlet is 77.50 mm.

Mesh

Unstructured mesh was employed for the domain with inflation layers added to wall surfaces. The mesh in the area in front of the nozzle is refined to capture any high gradients of the hydrodynamic variables.

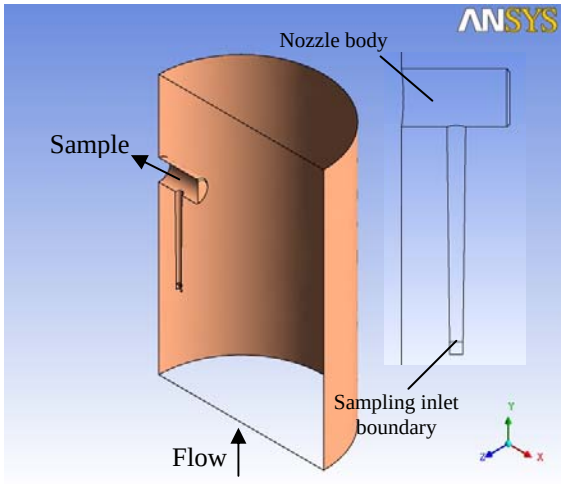

Figure 1: Ideal nozzle.

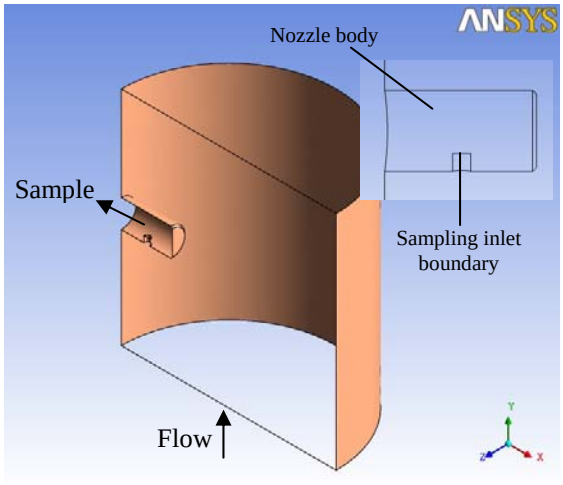

Figure 2: Nozzle A

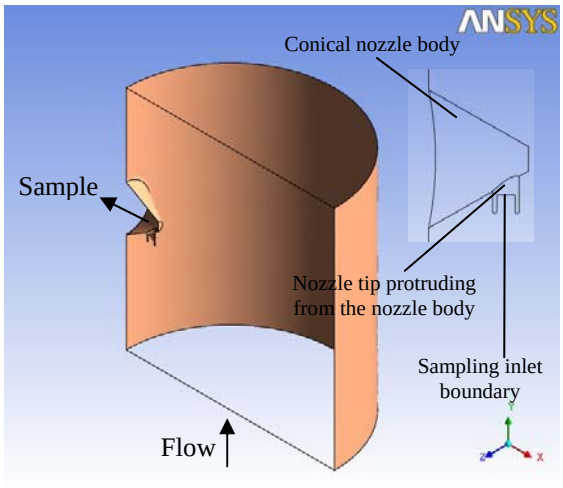

Figure 3: Nozzle B

Boundary Conditions

Fluid and particle conditions (e.g. velocity, turbulent intensity, volume fractions, etc.) entering the domains were imported from the outlet information of simulations of a long straight vertical pipe. This ensures that the flow is fully developed as it enters the domains, and saves iteration time. The fully-developed turbulent condition entering the domain is confirmed by the computed profile shown in Figure 4. The sampling outlet velocity was set at 4.420 mm inside the nozzle entering ports. Zero relative pressure was assigned at the outlet boundary condition of the main pipe.

Two types of fluid giving different properties were studied: supercritical steam at 580°C and 280 bar, and pressurized water at 325°C and 150 bar. These conditions are, respectively, found in advanced gas-fired power plants and nuclear power plants. The two conditions do not represent feed water (typically 140-220°C, 200-250 bar) or condensate (20-30°C, 5 bar), although these might be of interest. Nonetheless, from the two conditions in this study, extrapolations to such systems can be made. Properties of fluids were determined with local conditions using the IAPWS97 formulation.

Mono-dispersed, spherical magnetite particles with diameters of 0.5, 1 and 2 μm were used separately as suspended solid. The three sizes of particle employed in different runs were to allow the effect of inertia to be observed. A constant density of 5200 kg/m^3 was used for the magnetite particle.

Numerical Models

An Eulerian-Eulerian multiphase model was employed for analyses of magnetite concentrations, which were determined at the inlet, sampling nozzle outlet and the main outlet. The standard k-ε model with medium intensity was used as the turbulence model for the continuous fluid in this study because of its robustness. The Dispersed Phase Zero Equation was used as a turbulence model for the dispersed phase. The drag force exerted on the magnetite particles was modeled using the Schiller Naumann Drag Model. The buoyancy force was modeled by considering the difference in density between phases (although there was demonstrated to be no effect in this study). Particle volume fraction was set at 2×10^{-7}, equivalent approximately to 1 ppm. A concentration of 1 ppm might not realistically represent steam/water cycle conditions in power plants; however, to avoid expensive computation yet provide meaningful results, this concentration proved to be appropriate. Other settings required to run the simulations were assigned in accordance with the CFD modeling guidelines [10]. Interphase turbulent dispersion force in an Eulerian-Eulerian multiphase model was neglected.

Runs were considered successfully converged when the concentration ratio was stable and residues were below the target. Concentration ratio, monitored throughout the iteration, is the ratio between sampling and inlet concentrations. It indicates particle collection efficiency. Stable values of concentration ratio represent results of particular steady-state runs, and are plotted against the corresponding sampling velocities.

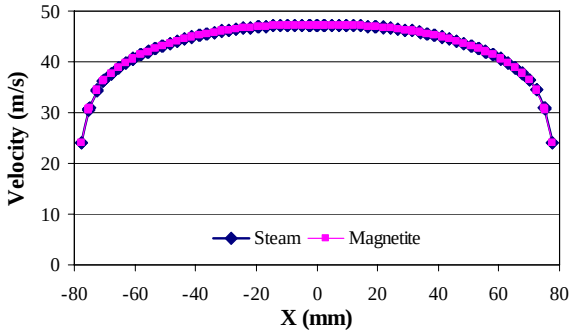

Figure 4: Velocity profile

Software Used

This study is performed using a commercial CFD program, ANSYS CFX 11.0, to simulate sampling collection efficiency for magnetite particles. Second-order spatial and temporal numerics are applied to the steady-state solution. Although a mesh independence study is not performed, various refinements such as inflation layers, along with a double precision solver, are used in several cases to ensure the accuracy and consistency of this model.

In addition to concentration ratio, fluid velocity and particle concentration distributions were also investigated. Particle deposition and release in the sample lines are not considered in this study.

Results and Discussion

Figures 5-8 show particle collection efficiency by plotting concentration ratio as a function of normalized sampling velocity, which is an area-averaged sampling velocity at the sampling outlet divided by an area-averaged mainstream velocity at the inlet. A concentration ratio of 1 indicates no deviation from the inlet concentration.

Figure 5 is a plot for 1-µm particles in the Ideal Nozzle in steam and pressurized water. It clearly shows that in steam, sampling concentration significantly depends on sampling velocity, whereas in pressurized water velocity has very little effect. This is because 1-µm particles follow the fluid streamline almost perfectly in pressurized water where viscous forces dominate. In steam, however, particle inertia is dominant and particles tend to follow their own path regardless of what the streamline does. As anticipated, sampling at lower than isokinetic rate results in concentration higher than the real value and vice versa. Here, sampling at 25% lower than the isokinetic velocity in steam results in a concentration 10% higher than the real value, and sampling at the isokinetic rate gives a representative result.

Figures 6-8 compare three different particle sizes sampled with the three different nozzles in steam. The effect of particle size on collection efficiency is clearly demonstrated. Smaller particles are able to adjust to a new condition of force better than larger ones. For the particle sizes considered in this study, practical nozzles can give satisfactory samples over a wide range of sampling velocities. Deviations from ideal sampling become greater for larger particle size. It is interesting to note that, as shown in Figures 7 and 8, if concentration ratio of unity is required from practical nozzles, sampling velocities higher than isokinetic rate should be employed. The effect of particle size, when sampling in pressurized water, can also be observed, but it is small, as shown in Figure 9. The difference in concentration ratio is not more than 2% within the range of sampling velocities studied.

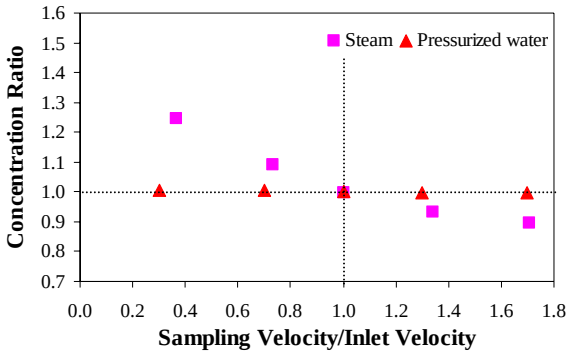

Figure 5: Ideal Nozzle, 1-µm particle

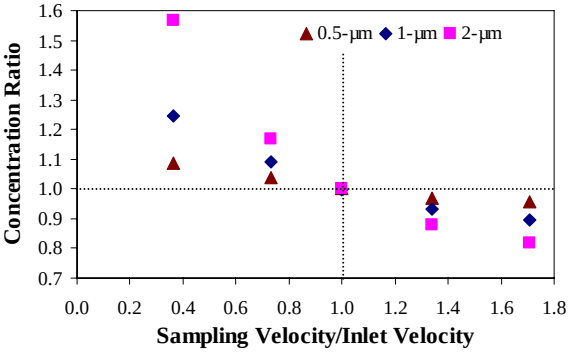

Figure 6: Ideal Nozzle in steam

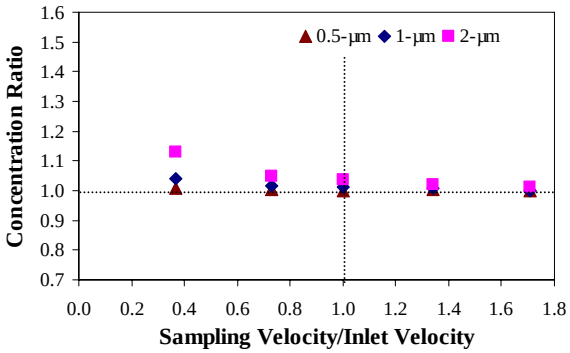

Figure 7: Nozzle A in steam

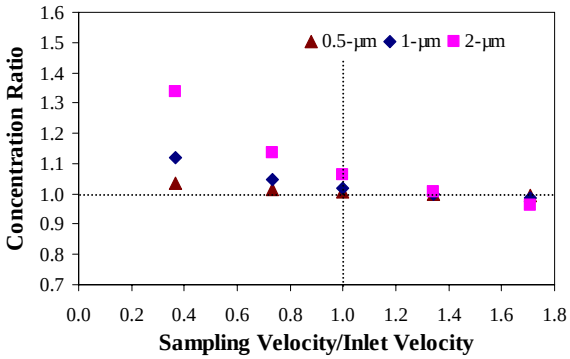

Figure 8: Nozzle B in steam

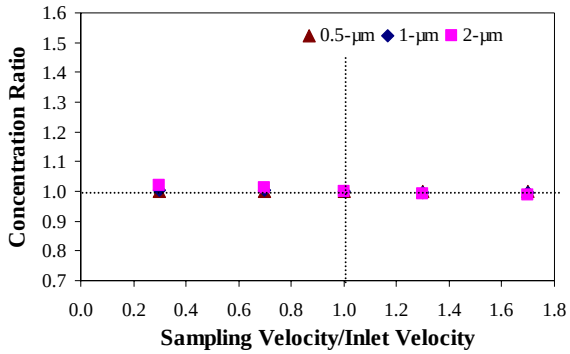

Figure 9: Ideal Nozzle in pressurized water

The effect of sampling nozzle on particle collection efficiency is of interest. Figure 10 shows this effect on the sampling of 1-µm particles in steam. The Ideal Nozzle behaves as expected; the concentration ratio decreases as sampling velocity increases, passing through unity at the isokinetic rate. The deviations from unity of concentration ratio when sampling with Nozzles A or B at the isokinetic rate are less than 2%. Higher deviations are expected for particles larger than 1 µm. Sampling with the Ideal Nozzle is the most sensitive to sampling velocity, followed by Nozzle B. Nozzle A is the least sensitive among the three since its concentration ratio does not fall below unity within the range of sampling velocities studied. Figure 10 also shows that for 1-µm particles, sampling using Nozzles A or B at any flow rate gives results as good as or better than those from the Ideal Nozzle.

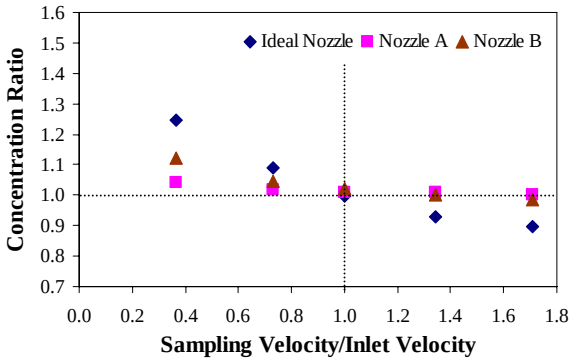

Figure 10: 1-µm particle in steam

This observation can be explained by contour plots as follows. Steam velocity contour plots of different nozzles on a symmetry plane sampled at different velocities are presented in Figures 11-13. It is evident that the nozzle bodies act as flow disturbances; the fluid is slowed down as it approaches the nozzle body. Nozzle A disturbs the flow field at the actual sampling point the most, followed by Nozzle B. Figure 11 shows that when sampled with the Ideal Nozzle, the body of fluid is extracted from the area where the velocity is the same as the average velocity, and where the flow field remains undisturbed. When sampling with Nozzles A and B, however, the fluid is actually extracted from the area where the velocities are lower than the average velocity. From Figures 12 and 13, the fluid velocities in front of entering ports of Nozzles A and B are about 20 m/s and 35 m/s, respectively. It is found that the flow field in front of the nozzles changes very little with sampling velocity.

With different nozzles, the body of fluid is extracted from the area in which fluid velocities are different, even though the sampling velocity is the same. This does not allow fluid to be sampled isokinetically in the cases of Nozzles A and B. To observe the effect of nozzle design better, Figures 14-16 show particle volume fraction distribution on a symmetry plane in steam sampled by different nozzles. They confirm that only the Ideal Nozzle samples the fluid from the 2×10^{-7} volume fraction region (bulk volume fraction), whereas Nozzles A and B draw samples from a higher volume fraction region. This higher volume fraction region is created by the fact that particles do not follow the fluid streamlines, which go around an obstacle. The fluid flux in front of the nozzle body reduces, while the particle flux remains virtually unchanged. Table 1 shows approximate steam velocities and magnetite volume fractions in front of the entering ports of the sampling nozzles.

Table 1: Steam velocities and magnetite volume fractions in pipe entrance and in front of entering ports of sampling nozzles

Location	Steam velocity (m/s)	Magnetite volume fraction
Pipe entrance	41	2.00×10^{-7}
Ideal Nozzle	41	2.00×10^{-7}
Nozzle A	20	2.08×10^{-7}
Nozzle B	35	2.08×10^{-7}

It should be noted that changing sampling velocity does not alter the volume fraction contour in front of the nozzle bodies. The higher volume fraction region is created mainly by the nozzle body. However, one can notice that the volume fraction contour inside the entering ports changes with sampling velocity, particularly in the case of Nozzle A. It seems that at higher sampling velocity, a higher particle concentration is drawn into the nozzle; this contradicts the observation made from Figures 5-10. This, however, can be explained as follows. Particle volume fraction is only indirectly related to concentration. Particle volume fraction is based on

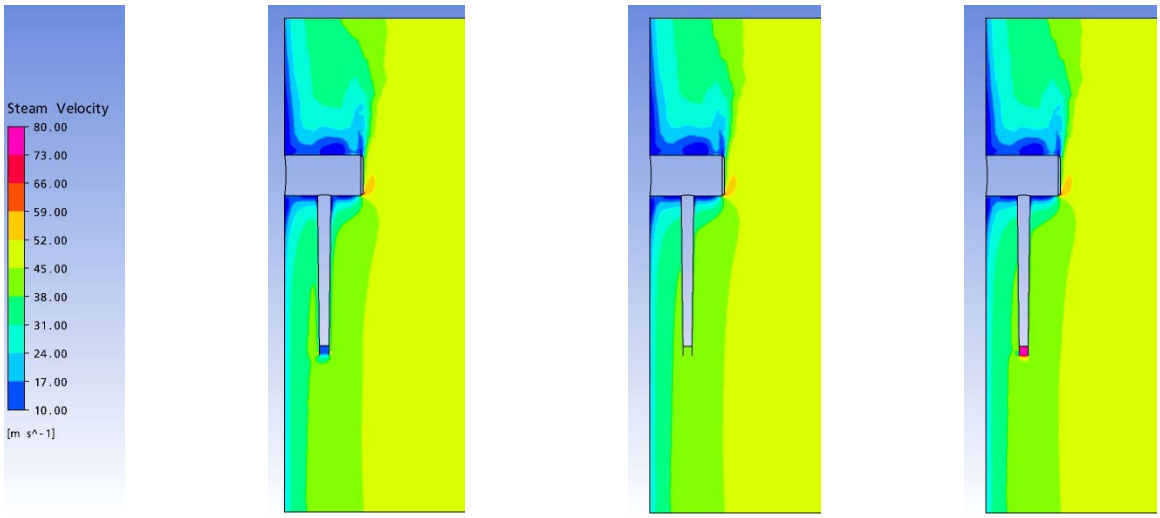

(a) (b) (c)

Figure 11: Velocity contour of steam on a symmetry plane from the wall to the center line when sampled with Ideal Nozzle at a) 15 m/s, b) 41 m/s (isokinetic rate), and c) 70 m/s

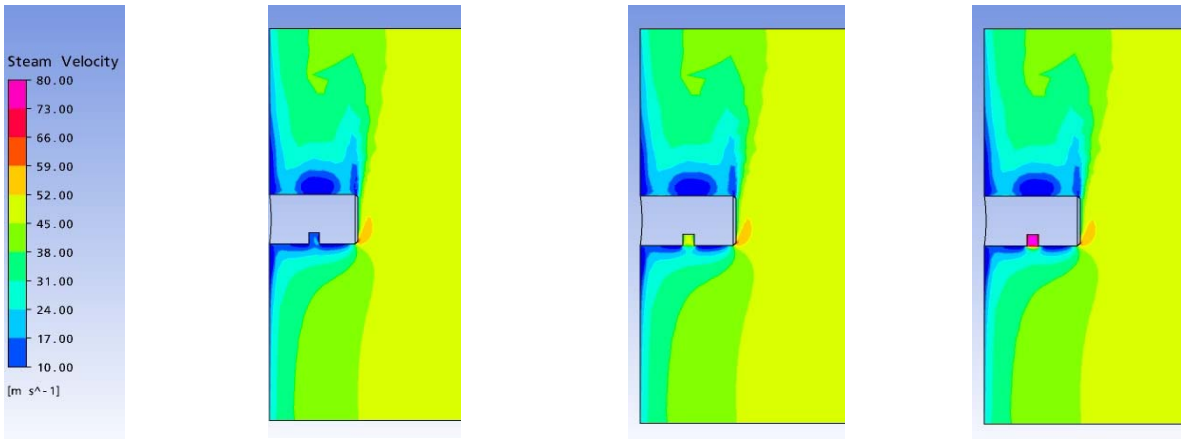

(a) (b) (c)

Figure 12: Velocity contour of steam on a symmetry plane from the wall to the center line when sampled with Nozzle A at a) 15 m/s, b) 41 m/s (isokinetic rate), and c) 70 m/s

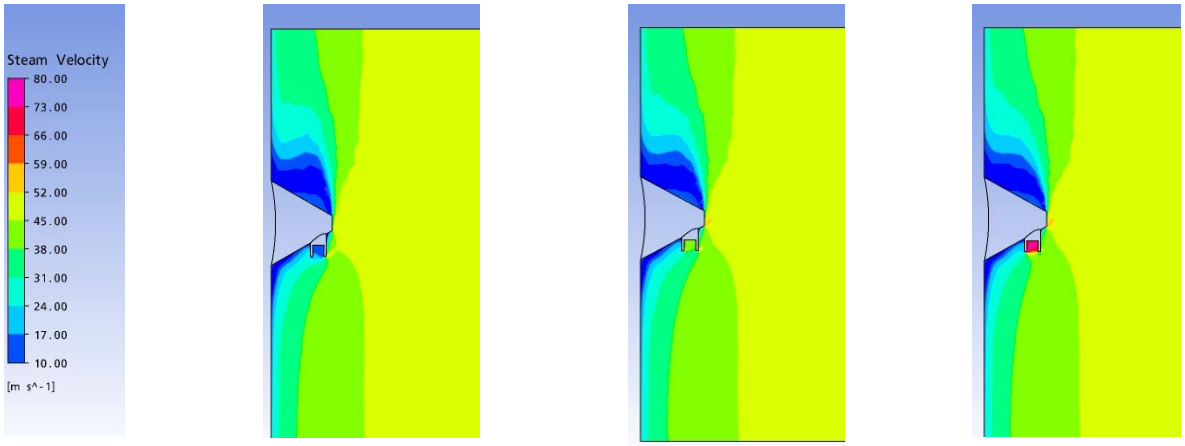

(a) (b) (c)

Figure 13: Velocity contour of steam on a symmetry plane from the wall to the center line when sampled with Nozzle B at a) 15 m/s, b) 41 m/s (isokinetic rate), and c) 70 m/s

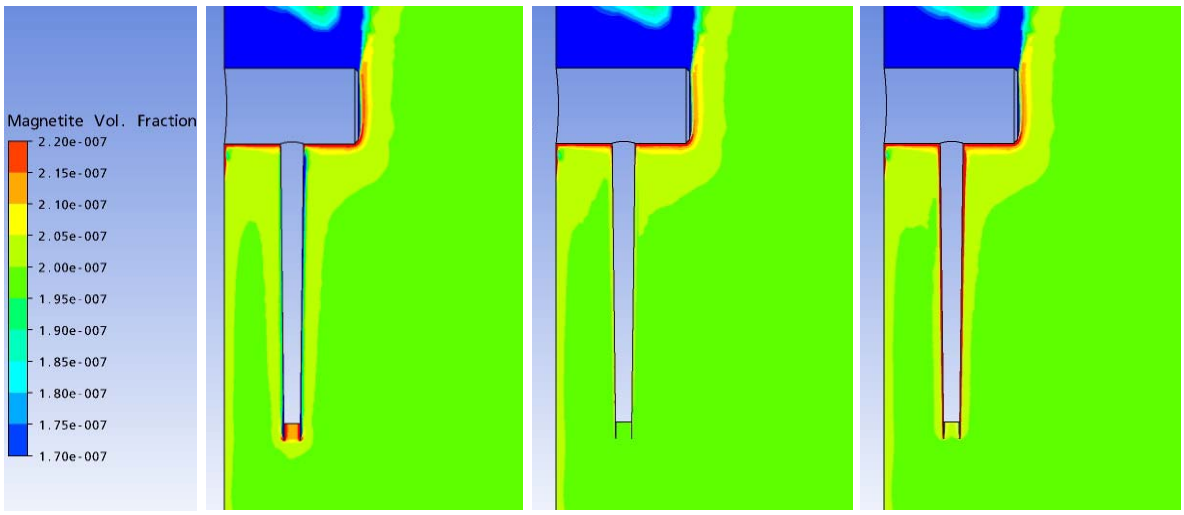

(a) (b) (c)

Figure 14: Particle volume fraction contour in steam on a symmetry plane sampled with Ideal Nozzle at a) 15 m/s, b) 41 m/s (isokinetic rate), and c) 70 m/s

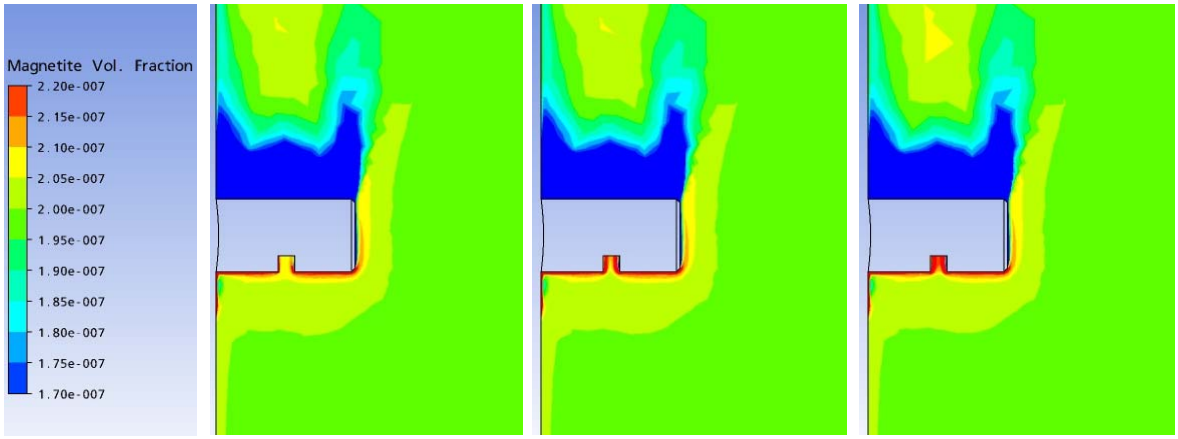

(a) (b) (c)

Figure 15: Particle volume fraction contour in steam on a symmetry plane sampled with Nozzle A at a) 15 m/s, b) 41 m/s (isokinetic rate), and c) 70 m/s

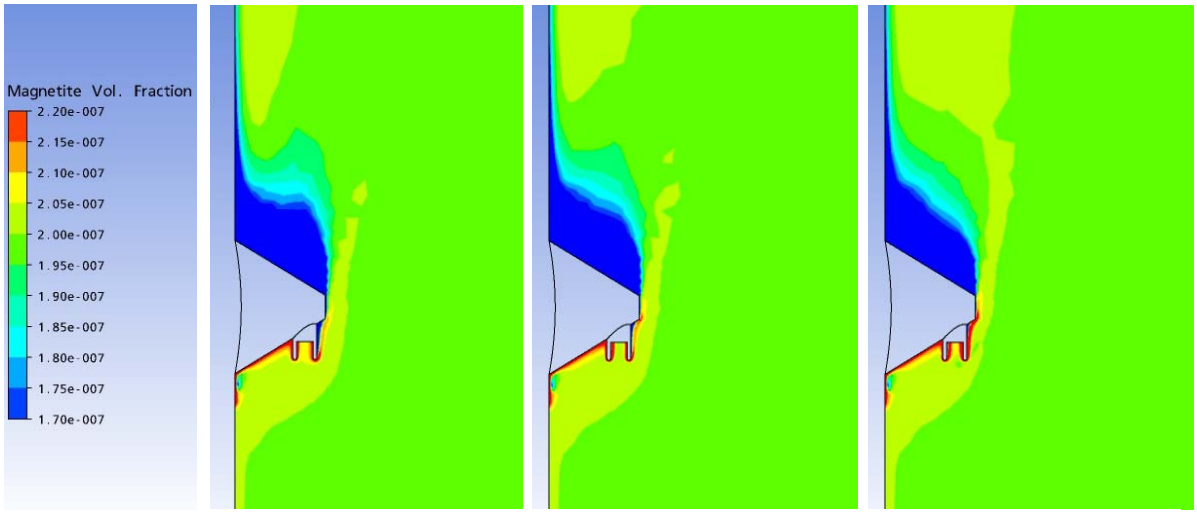

(a) (b) (c)

Figure 16: Particle volume fraction contour in steam on a symmetry plane sampled with Nozzle B at a) 15 m/s, b) 41 m/s (isokinetic rate), and c) 70 m/s

the volume in particular computation cells taken up by particles, and does not concern fluid velocity, which changes with sampling rate. At the sampling inlet, both particle and fluid mass flows increase with sampling velocity; however, particle concentration decreases because of the greater fluid flux. At high sampling velocity, more particles are drawn into the cell in the entering port and, hence, a high volume fraction results.

It is important to bear in mind that deviations of concentration ratio observed in this study are small compared with error commonly introduced by plant sampling practices, which can attain orders of magnitude. This is because sample line effects, which are believed, from plant experience, to be major sources of sampling deficiencies, are not considered here. These errors are all cumulative.

Conclusions

The simulations performed in this study are a theoretical analysis of sampling nozzle collection efficiency. The simulations reveal that for sampling magnetite particles from steam, where the fluid viscosity is low, the collection efficiency significantly depends on the sampling velocity. The degree of deviation from perfect sampling depends on particle size and sampling velocity. The simulations of sampling with the Ideal Nozzle show that concentration is overestimated when samples are taken at lower than the isokinetic rate and vice versa. It should be kept in mind that the Ideal Nozzle is hypothetical and cannot be made in practice. In liquid systems, sampling velocity has almost no effect within a range of parameters studied.

It is evident that any practical sampling nozzle for steam acts as an obstacle that disturbs the flow field and tends to remove the isokinetic condition. Despite the fact that Nozzle A creates the highest disturbance to the flow field among the three, the effect of sampling velocity on sampling concentration is the least. This is because the fluid approaching the nozzle is slowed down, creating a higher particle concentration region in front of the nozzle. This region is a direct effect of the nozzle body that disturbs the flow field and does not change significantly with sampling velocity. The nozzle, therefore, actually extracts fluid from a region that has a concentration higher than in the bulk. This results in sampling concentrations being less sensitive to sampling velocity than in the case of the Ideal Nozzle. In other words, for particle sizes considered in this study, practical nozzles can give satisfactory samples over a wide range of sampling velocities. However, it should be noted that deviations from ideal sampling become greater for larger particles. Therefore, it is advisable to be aware of this effect, and to extract samples at the appropriate velocity, particularly from steam. Effects in low-pressure steam are still to be investigated.

Acknowledgements

This paper is continuing work resulting from an International Collaboration sponsored by the International Association for the Properties of Water and Steam. Alstom, Switzerland and Dong Energy, Denmark are thanked for their support of the project.

References

[1] *P. Srisukvatananan, D.H. Lister, R. Svoboda, and K. Daucik:* Assessment of the State of the Art of Sampling of Corrosion Products from Water/Steam Cycles. Power Plant Chemistry, 9(10), 613-626 (2007).

[2] *S.K. Beal:* Deposition of Particles in Turbulent Flow on Channel or Pipe Walls. Nuclear Science and Engineering, 40, 1-11 (1970).

[3] Corrosion Product and Particulate Sampling from the Sizewell B PWR Primary Coolant. TEPDZ 35010, 1993. Nuclear Electric.

[4] Development of a Steam Sampling System. EPRI TR-100196, 1991. EPRI.

[5] Sampling Considerations for Monitoring Corrosion Products in the Reactor Coolant System in Pressurized Water Reactors. 1013668, 2006. EPRI.

[6] Standard Practice for Sampling Steam. ASTM D1066-97 (Reapproved 2001), 2001.

[7] Standard Practice for Sampling Steam. ASTM D1066-06, 2006.

[8] *R. Svoboda, G. Ziffermayer, S. Romanelli, W. Kaufamm, L. Sozzi, and M.E. Schaefer:* Trace Analysis of Corrosion Products by Integrating Sampling Techniques. in Water Chemistry of Nuclear Reactor Systems 3. Bournemouth, UK: BNES. (1983).

[9] *W.C. Hinds:* Aerosol Technology: Properties, Behavior and Measurement of Airborne Particles. 1982, NY: John Wiley & Sons.

[10] *ANSYS CFX-Solver Modeling Guide*, in *ANSYS CFX Release 11.0*. 2006.